Protonation Sites in Pyrimidine and Pyrimidinamines in the Gas Phase

Viet Q. Nguyen and František Tureček*

Contribution from the Department of Chemistry, Bagley Hall, Box 351700, University of Washington, Seattle, Washington 98195-1700

Received October 4, 1996[⊗]

Abstract: Protonation sites in gaseous pyrimidine (**1**), 2-pyrimidinamine (**2**), and 4-pyrimidinamine (**3**) were elucidated by neutralization−reionization mass spectrometry and MP2/6-311G(2d,p) ab initio calculations. Pyrimidine was protonated with NH_4^+ and t-$C_4H_9^+$ exclusively at the nitrogen atoms whose proton affinity (PA) was calculated at 879 kJ mol^{-1} in excellent agreement with the experimental datum. The C-2 and C-5 positions in **1** had PA = 573 and 645 kJ mol^{-1}, respectively. **2** was protonated with t-$C_4H_9^+$ at N-1 and/or N-3 and the amine group in a statistical 2:1 ratio, consistent with the calculated PA = 909 and 864 kJ mol^{-1}, respectively. **3** was protonated at N-1, N-3, and the amine group, which had PA = 943, 905, and 835 kJ mol^{-1}, respectively. The C-5 positions in **2** and **3** were less basic, PA = 807 and 781 kJ mol^{-1}, respectively, and were not attacked by the gas-phase acids used. The thermodynamic proton affinities of gaseous **1**, **2**, and **3** followed the order of their basicities in solution. The substituent electronic effects on the topical proton affinities are discussed. Pyrimidinium radicals derived from the tautomers of ring-protonated **1**, **2**, and **3** were found by MP2/6-311G(2d,p) and B3LYP/6-311G(2d,p) to be stable in their equilibrium geometries and upon formation by vertical electron transfer. An unusual kinetic stability was found for pyrimidinium radicals derived from N-1- and N-3-protonated **3**.

Introduction

The pyrimidine (**1**) ring is a structural motif that appears in a variety of biologically important molecules. 2-Pyrimidinamine (**2**) is incorporated in the molecules of, *inter alia*, guanine and folic acid, while 4-pyrimidinamine (**3**) is the building block of

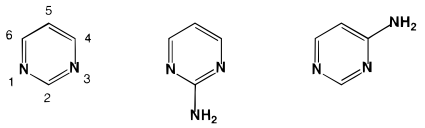

1 **2** **3**

adenine, cytosine, and thiamine. The physical properties of pyrimidine and pyrimidinamines have been studied extensively in solution but less so in the gas phase.[1] In particular, pyrimidine is a weak base in solution ($pK_{BH} = 1.3$)[2] and the gas phase, where it shows a proton affinity, PA = 881 kJ mol^{-1},[3,4] which is lower than those of pyridine and pyridazine, but higher than that of pyrazine.[4] Pyrimidinamines are somewhat stronger bases in solution where they show $pK_{BH} = 3.5-3.7$ and 5.7 for **2** and **3**, respectively.[5] Gas-phase proton affinities of pyrimidinamines are unknown. Orozco et al. used semiempirical calculations to estimate the proton affinity of the N-3 position in **3**.[6] Sindona et al. have recently estimated the gas-phase proton affinities of some pyrimidine and purine nucleosides from competitive dissociations of proton-bound dimers.[7]

In addition to the overall, thermodynamic basicity, determination of *protonation sites* in polyfunctional molecules has been of much interest. In particular, the site of protonation in DNA bases determines intermolecular hydrogen bonding in DNA−protein interactions and DNA and RNA coiling.[8] In solution, protonation sites in nitrogen heterocycles have been determined from ^{13}C and ^{15}N shifts in NMR spectra and modeled by theory.[9] The 4-pyrimidinamine system in cytosine was found to be protonated in the N-3 ring position in a D_2O solution,[10a] whereas 4-amino-2,6-dimethylpyrimidine was protonated at N-1.[10b−d] Different protonation sites have also been found in purine and adenine (N-1) on one hand and guanine (N-7 or N-9) on the other.[11]

Protonation in the gas phase occurs in the absence of solvent molecules, and its regiospecificity and thermodynamics can differ substantially from those observed in solution.[12] It is therefore of interest to investigate protonation sites in gas-phase molecules to gauge the intrinsic, solvent-effect-free basicities of the functional groups and their intramolecular interactions. Another salient feature of gas-phase protonation is that it can be conducted at various levels of exothermicity depending on the acid used (BH^+, eq 1). For a polyfunctional molecule (M),

$$M + BH^+ \rightleftarrows MH^+ + B \qquad (1)$$

the most basic site can be protonated selectively with a gas-

[⊗] Abstract published in *Advance ACS Abstracts,* February 15, 1997.

(1) Brown, D, J.; Evans, R. F.; Cowden, W. B.; Fenn, M. D. *The Pyrimidines*; Wiley-Interscience: New York, 1994.
(2) Brignell, P. J.; Johnson, C. D.; Katritzky, A. R.; Skakir, Tarhan, H. O.; Walker, G. *J. Chem. Soc. B* **1967**, 1233.
(3) Meot-Ner (Mautner), M. *J. Am. Chem. Soc.* **1979**, *101*, 2396.
(4) Lias, S. G.; Liebman, J. F.; Levin, R. D. *J. Phys. Chem. Ref. Data* **1984**, *13*, 695.
(5) (a) Albert, A.; Goldacre, R.; Phillips, J. N. *J. Chem. Soc.* **1948**, 2240. Brown, D. J.; England, B. T.; Lyall, J. M. *J. Chem. Soc. C* **1966**, 226. (c) Khromov-Borisov, N. V. *Dokl. Akad. Nauk SSSR* **1968**, *180*, 1129.
(6) Orozco, M.; Franco, R.; Mallol, J; Canela, E. I. *Bioorg. Chem.* **1990**, 361.
(7) Liguori, A.; Napoli, A; Sindona, G. *Rapid Commun. Mass Spectrom.* **1994**, *8*, 89.
(8) (a) Martin, K. B. In *Metal Ions Binding to Nucleosides*; Xavier, A. V., Ed.; VCH Publishers: Weinheim, 1986.
(9) (a) Giessner-Prettre, C.; Pullman, B. *J. Am. Chem. Soc.* **1982**, *104*, 70. (b) Ribas-Prado, F.; Giessner-Prettre, C. *J. Magn. Reson.* **1982**, *47*, 103. (c) Schindler, M. *J. Am. Chem. Soc.* **1988**, *110*, 6623.
(10) (a) Benoit, R. L.; Frechette, M. *Can. J. Chem.* **1986**, *64*, 2348. (b) Tewari, K. C.; Lee, J.; Li, N. C. *Trans. Faraday Soc.* **1970**, *66*, 2069. (c) Kim, S. H.; Martin, R. B. *Inorg. Chim. Acta* **1984**, *91*, 19. (d) Sovago, Martin, R. B. *Inorg. Chem.* **1980**, *19*, 2868.
(11) (a) Benoit, R. L.; Frechette, M. *Can. J. Chem.* **1984**, *62*, 995. (b) *Ibid.* **1985**, *63*, 3053.
(12) Bowers, M. T., Ed. *Gas-Phase Ion Chemistry;* Academic Press: New York, 1979; Vol. 2, pp 1−51.

S0002-7863(96)03478-6 CCC: $14.00

phase acid of matching proton affinity, and the conjugate acid MH^+ can be deprotonated with a suitable base. This approach was developed by Houriet and co-workers[13] and used recently by Kenttamaa and co-workers to determine the protonation sites in gaseous aniline.[14] In highly exothermic protonations with strong gas-phase acids, such as CH_5^+, H_3O^+, or t-$C_4H_9^+$, which are often used in chemical ionization mass spectrometry,[15] polyfunctional molecules can be protonated at different basic sites to yield isomeric cations. These can exist as separate isomers or interconvert by intramolecular proton transfer under unimolecular conditions[16] or by an ion molecule reaction with M. Protonation exothermicity and other experimental conditions (reagent gas pressure, temperature, ion residence time, etc.) therefore can have an effect on the composition of ion isomers produced by exothermic protonation.[17] To determine the protonation site(s), isolated ions must be studied under conditions preventing bimolecular encounters or surface catalysis. However, unimolecular dissociations of closed-shell cations are often nonspecific in that they require high threshold or activation energies and are preceded by intramolecular proton migrations that can obliterate the original position of the proton introduced by the gas-phase acid.[18]

We have shown recently,[16,19] following the previous work of Harrison and co-workers,[20] that protonation sites in heterocycles can be determined by combination of variable-time neutralization−reionization mass spectrometry[21] and deuterium labeling. In this method, stable cations produced by exothermic protonation are neutralized by fast electron transfer from gas-phase molecules under single-collision conditions. Thermal organic molecules are used as electron donors in what is essentially a nonresonant electron transfer.[22] Due to the very short interaction time ($\sim 10^{-15}$ s), the radical formed has the same structure as the precursor cation, so that the C−H or N−H bonds due to proton attachment in the precursor cation (MH^+) are preserved in the radical ($MH^\bullet$). However, the radicals are typically less stable than their cation precursors, and a fraction dissociate unimolecularly by loss of hydrogen or substituents or by a ring cleavage.[16,19] To determine the protonation site in the cation, the incoming proton from BH^+ and the hydrogens in the substrate molecule (M) are distinguished by labeling. Deuteronation of a methine or an amino group, followed by collisional neutralization, results in losses of both H and D atoms from the intermediate radicals (Scheme 1). By contrast, deuteronation of an imine nitrogen atom results in the loss of the deuterium atom. The products are distinguished and monitored by mass spectrometry following collisional reionization of the neutral products to cations or cation radicals. If a fraction of radicals survives and is reionized to MH^+, nonspecific ion dissociations can occur whose products are

Scheme 1

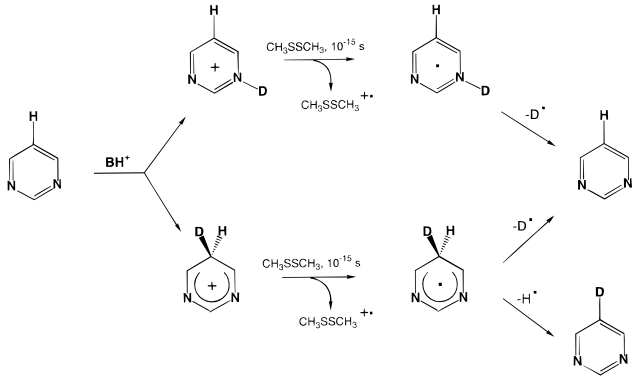

superimposed with those from radical dissociations, thus obscuring the latter. In such a case, neutral and ion dissociations can be distinguished by variable-time spectra in which the observation times for the radicals and ions are varied simultaneously within a 4×10^{-7} to 5×10^{-6} s range.[19,21]

Reduction of protonated heterocycles gives rise to radicals whose stabilities and unimolecular dissociations are of interest. Radicals derived from the related DNA bases have been studied extensively in conjunction with their role in radiation damage.[23] While several hydroxyl radical adducts have been identified through their stable secondary products,[23] hydrogen atom adducts have been more difficult to study because of their high reactivity.[24] Heterocyclic radicals are also presumed but not proven as reactive intermediates in the electrochemical reduction of pyridinium cations in aprotic solution.[25] Neutralization−reionization mass spectrometry[26] is a straightforward methodology for studying such elusive radical intermediates and hydrogen atom adducts, which are generated readily in an isolated state by vertical neutralization of protonated heterocycles in the rarefied gas phase. In this work we combine neutralization−reionization methods and ab initio calculations to determine the protonation sites in gaseous pyrimidine and pyrimidinamines **2** and **3** to estimate the relevant proton affinities, to assess the stabilities of the intermediate radicals, and to identify their dissociation products.

Experimental Section

Measurements were made on a tandem quadrupole acceleration−deceleration mass spectrometer described previously.[27] Cation radicals were prepared by electron impact ionization at 70 eV. Gas-phase protonations were carried out with CH_5^+/CH_4, H_3O^+/H_2O, t-$C_4H_9^+/i$-C_4H_{10}, and NH_4^+/NH_3, and deuteronations with D_3O^+/D_2O, t-$C_4D_9^+/i$-C_4D_{10}, and ND_4^+/ND_3. The reagent gas pressure in the ion source, estimated at 0.1−0.2 Torr, was adjusted to maximize the peak of the protonated or deuteronated heterocycle and suppress the formation of cation radicals to achieve abundance ratios $[M + H, D]^+/[M^{\bullet+}] > 10$ in most instances. In this way, contamination by isobaric overlaps of ^{13}C and ^{15}N satellites of the stable heterocycle ions was minimized at

(13) (a) Houriet, R.; Schwarz, H. *Lect. Notes Chem.* **1982**, *31*, 229. (b) Houriet, R.; Schwarz, H.; Zummack, W.; Andrade, J. G.; Schleyer, P. v. R. *New J. Chem.* **1981**, *5*, 505.

(14) Smith, R. L.; Chyall, L. J.; Beasley, B. J.; Kenttamaa, H. I. *J. Am. Chem. Soc.* **1995**, *117*, 7971.

(15) Harrison, A. G. *Chemical Ionization Mass Spectrometry*, 2nd ed.; CRC Press: Boca Raton, FL, 1992.

(16) Nguyen, V. Q.; Turecek, F. *J. Mass Spectrom.* **1996**, *31*, 1173.

(17) Tkaczyk, M.; Harrison, A. G. *Int. J. Mass Spectrom. Ion Processes* **1994**, **132**, 73 and references therein.

(18) (a) Maquestiau, A.; Van Haverbeke, Y.; Mispreuve, H.; Flammang, R.; Harris, J. A.; Howe, I.; Beynon, J. H. *Org. Mass Spectrom.* **1980**, *15*, 144. (b) Wood, K. V.; Burinsky, D. J.; Cameron, D.; Cooks, R. G. *J. Org. Chem.* **1983**, *48*, 5236.

(19) Nguyen, V. Q.; Turecek, F. *J. Mass Spectrom.* **1997**, *32*, 55.

(20) McMahon, A. W.; Chadikun, F.; Harrison, A. G.; March, R. E. *Int. J. Mass Spectrom. Ion Processes* **1989**, *87*, 275.

(21) (a) Kuhns, D. W.; Tran, T. B.; Shaffer, S. A.; Turecek, F. *J. Phys. Chem.* **1994**, *98*, 4845. (b) Kuhns, D. W.; Turecek, F. *Org. Mass Spectrom.* **1994**, *29*, 463.

(22) Holmes, J. L. *Mass Spectrom. Rev.* **1989**, *8*, 513.

(23) (a) Sevilla, M. D.; Becker, D. *R. Soc. Chem. Spec. Rev., Electron Spin Reson.* **1994**, *14*, 130. (b) Becker, D.; Sevilla, M. D. In *Advances in Radiation Biology*; Lett, J. T., Adler, H., Eds.: Academic Press: New York, 1993; p 121. (c) Steenken, S. *Chem. Rev.* **1989**, *89*, 503.

(24) Deeble, D. J.; von Sonntag, C. *Int. J. Radiat. Biol.* **1984**, *49*, 247. (b) Scholes, G.; Simic, M. *Biochim. Biophys. Acta* **1986**, *166*, 255. (c) Das, S.; Deeble, D. J.; von Sonntag, C. *Z. Naturforsch., Sect. C* **1985**, *40C*, 292. (d) Candeias, L. P.; Steenken, S. *J. Phys. Chem.* **1992**, *96*, 937.

(25) Ludvik, J.; Turecek, F.; Volke, J. *J. Electroanal. Chem.* **1985**, *188*, 105.

(26) For recent reviews see (a) Goldberg, N.; Schwarz, H. *Acc. Chem. Res.* **1994**, *27*, 347. (b) Turecek, F. *Org. Mass Spectrom.* **1992**, *27*, 1087. (c) McLafferty, F. W. *Int. J. Mass Spectrom. Ion Processes* **1992**, *118/119*, 221.

(27) Turecek, F.; Gu, M.; Shaffer, S. A. *J. Am. Soc. Mass Spectrom.* **1992**, *3*, 493.

≤0.5%. Stable ions of 78 eV kinetic energy and 32−34 μs lifetimes were accelerated to 8200 eV and neutralized by collisions with thermal dimethyl disulfide, which was admitted to the neutralization cell at pressures such as to achieve 70% transmittance of the precursor ion beam. This corresponded to mostly (~85%) single-collision conditions. The residual ions were reflected by an electrode maintained at +250 V, and the neutral intermediates were reionized to cations by collisions with oxygen which was admitted into the vacuum system at pressures such as to achieve 70% transmittance of the precursor ion beam. Reionization in the collision cell sampled neutral intermediates of 4.4−4.8 μs. Variable-time reionization in a floated ion conduit between the neutralization and reionization cells[21] sampled neutrals at observation times that were varied between 0.4 and 3.0 μs depending on the particle velocity.

Calculations

Standard ab initio calculations were carried out using the Gaussian 92 suite of programs.[28] Geometries were optimized with Hartree−Fock calculations using the 6-31G(d,p) basis set. Harmonic frequencies were obtained from HF/6-31G(d,p) calculations and scaled by 0.893 to provide zero-point corrections.[29] The corrected harmonic frequencies were also employed to calculate thermodynamic functions using the rigid-rotor, harmonic-oscillator approximation. The optimized geometries in Cartesian coordinates and the uncorrected harmonic frequencies are available as Supporting Information. To account in part for electron correlation effects, single-point calculations were performed with the larger 6-311G(2d,p) basis set[30] using the Møller−Plesset perturbational treatment[31] which was truncated at second order (MP2) with frozen core excitations.[28] MP2 calculations with spin-unrestricted wave functions gave spin values ($\langle S^2 \rangle$) that in some cases exceeded those expected for doublets (0.75) and indicated contamination with higher quartet states. These higher-spin contributions were in part annihilated[32] using Schlegel's spin projection method.[33] Alternatively, single-point calculations were carried out using the density-functional theory,[34] which was recently shown to give reliable energies for radical dissociations and avoid spin contamination problems.[35,36] Becke's B3LYP hybrid method[37] was applied, which used a three-parameter functional with Vosko, Wilk and Nusair's local correction functional,[38] and a nonlocal correction according to Lee, Yang, and Parr.[39] Charge distributions (total atomic charges) and total spin densities were obtained from Mullikan population analysis of the UHF/6-311G(2d,p) wave functions and B3LYP/6-311G(2d,p) density matrices.

Results and Discussion

Protonation of Pyrimidine. The properties of radicals related to pyrimidinamines were first investigated with the parent pyrimidine system (**1**). Protonations of **1** with gas-phase H_3O^+ and NH_4^+ were exothermic,[40,41] according to eqs 2 and 3 and

$$\mathbf{1} + H_3O^+ \rightarrow (\mathbf{1} + H)^+ + H_2O \qquad \Delta H_r = -192 \text{ kJ mol}^{-1} \tag{2}$$

$$\mathbf{1} + NH_4^+ \rightarrow (\mathbf{1} + H)^+ + NH_3 \qquad \Delta H_r = -29 \text{ kJ mol}^{-1} \tag{3}$$

formed stable pyrimidinium ions, $(\mathbf{1} + H)^+$. Ions $(\mathbf{1} + H)^+$ prepared according to eqs 2 and 3 differed in their internal energies due to the different protonation exothermicities, but were stable with respect to unimolecular dissociation. This was inferred from the chemical ionization mass spectra that showed $(\mathbf{1} + H)^+$ as the only ion species formed by protonation with H_3O^+ and NH_4^+. It was also consistent with thermochemical data that predicted highly endothermic dissociations for $(\mathbf{1} + H)^+$; for example, the reaction $(\mathbf{1} + H)^+ \rightarrow \mathbf{1}^{\bullet+} + H^\bullet$ requires 460 kJ mol^{-1} at the thermochemical threshold.[42,43]

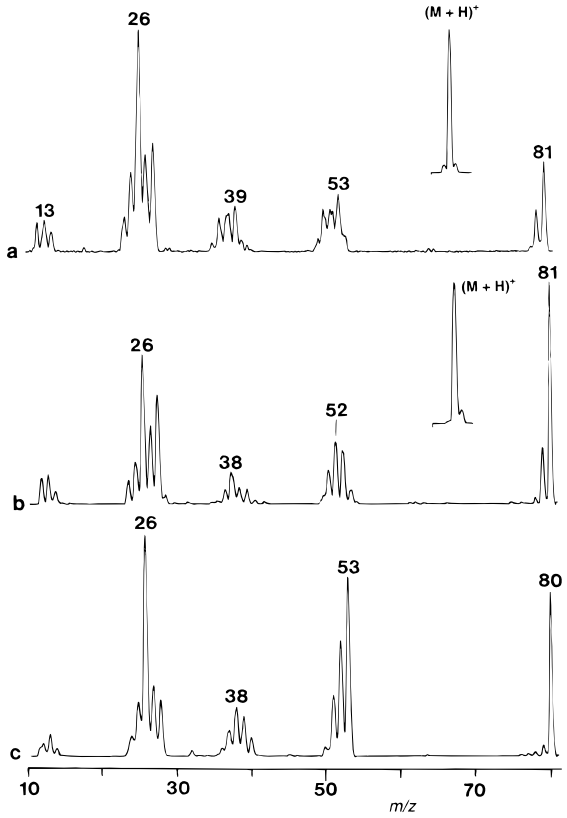

Figure 1. Neutralization (CH_3SSCH_3, 70% transmittance)−reionization (O_2, 70% transmittance) mass spectra of (a) pyrimidine protonated with H_3O^+, (b) pyrimidine protonated with NH_4^+, and (c) pyrimidine cation radical. Insets show the $(\mathbf{1} + H)^+$ precursor ion relative intensities.

Neutralization of $(\mathbf{1} + H)^+$ produced a fraction of stable pyrimidinium radicals, $(\mathbf{1} + H)^\bullet$ that gave rise to abundant survivor $(\mathbf{1} + H)^+$ ions following collisional reionization (Figure 1). The fraction of survivor ions clearly depended on the internal energy of the precursor $(\mathbf{1} + H)^+$ cations, as those formed by the milder protonation with NH_4^+ produced a larger fraction of survivor ions following neutralization and reionization. Loss of hydrogen was an important dissociation of $(\mathbf{1} + H)^\bullet$, which was used to probe the protonation site in $(\mathbf{1} + H)^+$ according to Scheme 1. $(\mathbf{1} + D)^+$ ions prepared by gas-phase deuteronation with D_3O^+ and ND_4^+ gave the neutralization−reionization spectra shown in Figure 2. Both spectra showed

(28) Frisch, M. J.; Trucks, G. W.; Head-Gordon, M.; Gill, P. M. W.; Wong, M. W.; Foresman, J. B.; Johnson, B. G.; Schlegel, H. B.; Robb, M. A.; Replogle, E. S.; Gomperts, R.; Andres, J. L.; Raghavachari, K.; Binkley, J. S.; Gonzalez, C.; Martin, R. L.; Fox, D. J.; DeFrees, D. J.; Baker, J.; Stewart, J. J. P.; Pople, J. A. *Gaussian 92/DFT, Revision C*; Gaussian Inc.: Pittsburgh, PA, 1993.
(29) Hehre, W. J.; Radom, L.; Schleyer, P. v. R.; Pople, J. A. *Ab Initio Molecular Orbital Theory*; Wiley: New York, 1986.
(30) Pople, J. A.; Head-Gordon, M.; Raghavachari, K. *J. Chem. Phys.* **1987**, *87*, 5968.
(31) Møller, C.; Plesset, M. S. *Phys. Rev.* **1934**, *46*, 618.
(32) Mayer, I. *Adv. Quantum Chem.* **1980**, *12*, 189.
(33) Schlegel, H. B. *J. Chem. Phys.* **1986**, *84*, 4530.
(34) Parr, R. G.; Yang, W. *Density-Functional Theory of Atoms and Molecules*; Oxford University Press: New York, 1989.
(35) Jursic, B. S. *Chem. Phys. Lett.* **1996**, *256*, 603.
(36) Jensen, G. M.; Goodin, D. B.; Bunte, S. W. *J. Phys. Chem.* **1996**, *100*, 954.
(37) Becke, A. D. *J. Chem. Phys.* **1993**, *98*, 5648.
(38) Vosko, S. H.; Wilk, L.; Nusair, M. *Can. J. Phys.* **1980**, *58*, 120.
(39) Lee, C.; Yang, W.; Parr, R. G. *Phys. Rev. B* **1988**, *37*, 785.
(40) From the proton affinities (kJ mol^{-1}) of pyrimidine (882), ref 4, water (690), and ammonia (853), ref 41.
(41) (a) Szulejko, J. E.; McMahon, T. B. *J. Am. Chem. Soc.* **1993**, *115*, 7839. (b) Szulejko, J. E. Revised Proton Affinity Data, University of Waterloo, April 1996.
(42) From the corresponding heats of formation (kJ mol^{-1}) of $(\mathbf{1} + H)^+$ (846), $\mathbf{1}^{\bullet+}$ (1087), and $H^\bullet$ (219) from ref 43.
(43) Lias, S. G.; Liebman, J. F.; Levin, R. D.; Kafafi, S. A. *NIST Standard Reference Database 19A*; National Institute of Standards and Technology: Gaithersburg, MD, 1993.

that loss of D was favored, as expressed by the [*m/z* 80]/[*m/z* 81] ratios, which were 18.7 and 3.3 for $(\mathbf{1} + D)^+$ prepared by deuteronation with D_3O^+ and ND_4^+, respectively. Hence, somewhat paradoxically, the radicals prepared from the more energetic $(\mathbf{1} + D)^+$ ions showed a more regiospecific loss of D.

Variable-time measurements were further used to gauge the time dependence of the H/D loss from $(\mathbf{1} + D)^\bullet$ generated from ND_4^+-deuteronated $(\mathbf{1} + D)^+$. The corresponding [*m/z* 80]/[*m/z* 81] ratios showed a steady *decrease* of D loss specificity upon increasing the ion observation time (τ_i) while decreasing the neutral observation time (τ_N), [*m/z* 80]/[*m/z* 81] = 2.1, 2.6, and 3.3 for τ_N = 0.4, 2.0, and 4.3 μs, respectively. The energy and time dependence of the H/D loss allowed a straightforward interpretation of the spectra. The $(\mathbf{1} + D)^+$ ions sampled for neutralization were predominantly (>98%) deuteronated on nitrogen, corresponding to structure $\mathbf{1a}^+$. Energetic radicals formed from $\mathbf{1a}^+$ dissociated *specifically* by losing the N-bound deuterium to form **1**. The nondissociating radicals were reionized to $\mathbf{1a}^+$, a fraction of which underwent *nonspecific* H/D loss that involved hydrogen and deuterium atoms regardless of their original positions. The H/D loss may have proceeded after hydrogen scrambling in the dissociating ions to yield $\mathbf{1}^{\bullet+}$, or by competitive H/D losses to form ylide tautomers of $\mathbf{1}^{\bullet+}$.[44] Note, however, that these postreionization ion dissociations, whose mechanisms were not resolved by the present experiments, did not interfere with the determination of protonation sites in **1**, as the latter followed unambiguously from the time-resolved, specific dissociations of the radical intermediates. Deuterium labeling also indicated that radical isomerizations, e.g., $\mathbf{1a}^\bullet \rightarrow \mathbf{1b,c}^\bullet$, did not precede the hydrogen loss, as $\mathbf{1b}^\bullet$ and $\mathbf{1c}^\bullet$ would eliminate both H and D if formed from $(\mathbf{1} + D)^\bullet$.

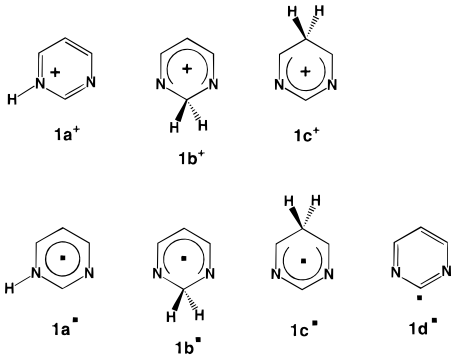

The experimental finding of specific N-protonation in gaseous **1** was in keeping with the previous studies of pyrimidine protonation in solution.[1] To obtain quantitative data regarding the topical proton affinities in gaseous **1** and the stabilities of the radical intermediates, we carried out ab initio calculations for several relevant species as summarized in Tables 1−3. MP2 calculations using basis sets with triply split valence shells and multiple sets of polarization functions have been shown previously to provide reliable estimates of proton affinities within ±5 kJ mol^{-1} of experimental values for a series of aromatic and aliphatic amines[45] and nitrogen heterocycles.[16,19] The present MP2/6-311G(2d,p) calculations, using HF/6-31G(d,p) zero-point and thermal enthalpy corrections (Table 1), gave the proton affinities in **1** as shown in Table 2. In line with experiment, the nitrogen atoms were the most basic sites in **1**,

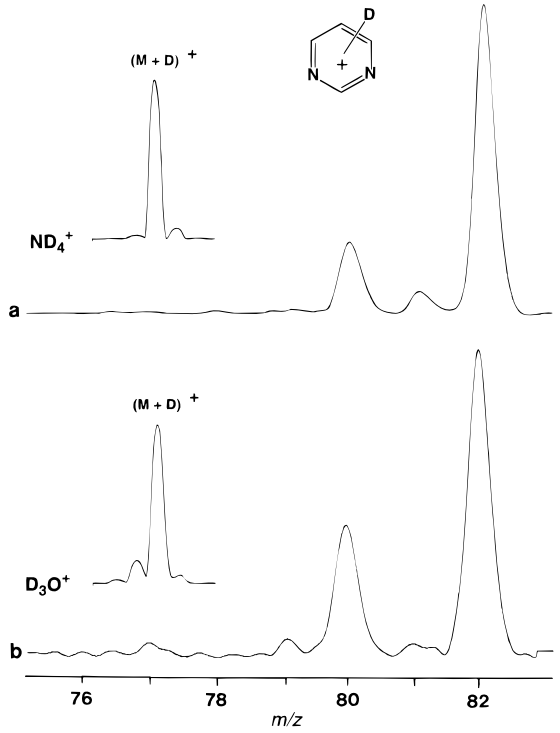

Figure 2. Partial NR mass spectra of deuteronated pyrimidine from deuteronations with (a) ND_4^+ and (b) D_3O^+. The collision conditions were as in Figure 1. Insets show the $(\mathbf{1} + D)^+$ precursor ion relative intensities.

so that $\mathbf{1a}^+$ was the most stable ion isomer. This finding was not very surprising in light of the fact that $\mathbf{1a}^+$ was the only isomer with an unperturbed aromatic π-electron system. The calculated proton affinity for N-1 or N-3 (879 kJ mol^{-1}) was in excellent agreement with the experimental value obtained by Mautner from high-pressure measurements[3] and converted to the proton affinity scale (882 kJ mol^{-1}).[4] The C-2 and C-5 positions were found to be substantially less basic, making ion tautomers $\mathbf{1b}^+$ and $\mathbf{1c}^+$ 306 and 234 kJ mol^{-1}, respectively, less stable than $\mathbf{1a}^+$. The calculated proton affinities further showed that, in keeping with the foregoing experimental results, these positions should not be attacked by H_3O^+ or NH_4^+. The topical proton affinity of C-4 was not calculated. C-4, which is an ortho−para position with respect to the ring nitrogen atoms, can be expected to have a proton affinity close to that of the ortho−ortho position C-2, but below that of the meta−meta position C-5. Protonation at C-4 was therefore deemed insignificant in gaseous **1**.

Pyrimidinium Radicals. Radicals $\mathbf{1a}^\bullet$−$\mathbf{1c}^\bullet$ correspond to products of hydrogen atom addition to the pyrimidine nucleus. $\mathbf{1a}^\bullet$ was found to be thermodynamically stable in its equilibrium geometry or when formed by vertical neutralization of cation $\mathbf{1a}^+$. The optimized geometries of $\mathbf{1a}^+$ and $\mathbf{1a}^\bullet$, which are given as Supporting Information, differed in their ring parameters. In particular, $\mathbf{1a}^\bullet$ showed elongation of the N-1−C-2 and N-1−C-6 bonds and pyramidalization at N-1. The ring in $\mathbf{1a}^\bullet$ was only slightly puckered, so that the pyramidalization at N-1 was mainly due to the out-of-plane deflection of the N-1−H-1 bond. These and the other small differences in the bond lengths and angles resulted in Franck−Condon effects in vertical neutralization, which amounted to 23 and 22 kJ mol^{-1} by MP2 and B3LYP calculations, respectively. Vertically neutralized $\mathbf{1a}^\bullet$ was formed with a planar geometry and shorter N−C bonds, so that the vibrational excitation was originally deposited as potential energy in the out-of-plane deformation (δ_{N-H} = 375 cm^{-1}), ring breathing (562, 630, 897, 952, 1010, and 1081

(44) (a) Hrusak, J.; Schroder, D.; Weiske, T.; Schwarz, H. *J. Am. Chem. Soc.* **1993**, *115*, 2015. (b) Lavorato, D.; Terlouw, J. K.; Dargel, T. K.; Koch, W.; McGibbon, G. A.; Schwarz, H. Unpublished results.

(45) Hillebrand, C.; Klessinger, M.; Eckert-Maksic, M.; Maksic, Z. B. *J. Phys. Chem.* **1996**, *100*, 9698.

Table 1. Ab Initio Energies

species	energy[a] HF/6-31G(d,p)	MP2/6-311G(2d,p)	$\langle S^2\rangle$[b]	B3LYP/6-311G(2d,p)	$\langle S^2\rangle$[b]	ZPVE[c]	$H_{298} - H_0$[c,d]
1	−262.700 342	−263.676 959	0	−264.394 756	0	194	13.6
1a$^+$	−263.062 517	−264.024 620	0			228	14.1
1b$^+$	−262.941 844	−263.904 296	0			217	15.2
1c$^+$	−262.987 784	−263.932 343	0			217	16.0
1d$^\bullet$	−262.058 840	−262.961 947	1.28	−263.713 072	0.76	158	13.8
		−262.992 576	1.0				
1a$^\bullet$	−263.248 561	−264.196 099	1.08	−264.954 297	0.77	213	16.3
		−264.217 665	0.82				
1a$^\bullet$ (VN)[e]		−264.188 414	1.06	−264.946 065	0.77	(228)[f]	
		−264.208 927	0.81				
1b$^\bullet$ (VN)[e]		−264.170 850	1.16	−264.936 179	0.78	(217)[f]	
		−264.199 129	0.86				
2	−317.755 035	−318.931 429	0	−319.787 360	0	237	17.5
2a$^+$	−318.130 176	−319.290 731	0			271	17.7
2b$^+$	−318.101 223	−319.274 320	0			272	18.3
2c$^+$	−318.098 175	−319.250 938	0			268	17.9
2a$^\bullet$	−318.297 427	−319.454 572	0.97	−320.340 652	0.77	259	19.3
		−319.469 745	0.77				
2a$^\bullet$ (VN)[e]		−319.438 820	0.93	−320.323 389	0.77	(271)[f]	
		−319.450 882	0.76				
2b$^\bullet$ (VN)[e]		−319.393 941	0.89	−320.270 240	0.76	(272)[f]	
		−319.404 332	0.76				
3	−317.751 941	−318.928 784	0	−319.784 238	0	237	17.5
3a$^+$	−318.139 451	−319.301 651	0			273	17.3
3b$^+$	−318.124 343	−319.286 306	0			271	17.7
3c$^+$	−318.086 215	−319.260 406	0			272	18.2
3d$^+$	−318.085 463	−319.238 125	0			267	18.4
3a$^\bullet$ (VN)[e]		−319.416 915	1.07	−320.311 920	0.77	(273)[f]	
		−319.438 417	0.98				
3b$^\bullet$ (VN)[e]		−319.419 654	1.01	−320.312 121	0.76	(271)[f]	
		−319.437 073					
NH_3	−56.211560	−56.420 161	0	−56.576 898	0	86	10.0
H$^\bullet$		−0.499 810	0	−0.502 156	0.75	0	6.2

[a] In units of hartrees, 1 hartree = 2625.5 kJ mol^{-1}. [b] Spin projected values in lower lines. [c] From HF/6-31G(d,p) harmonic frequencies scaled by 0.893; kJ mol^{-1}. [d] Enthalpy corrections for vibrational, rotational, and translational contributions at 298 K. [e] Single-point calculations on optimized ion geometries. [f] Zero-point energies in vertically neutralized radicals were arbitrarily taken equal to those in the corresponding ions.

Table 2. Proton Affinities[a]

protonation site	proton affinity	protonation site	proton affinity
	Pyrimidine		
N (**1a**$^+$)	879 (882)[b]	C-5 (**1c**$^+$)	645
C-2 (**1b**$^+$)	573		
	2-Pyrimidinamine		
N-1 (**2a**$^+$)	909	C-5 (**2c**$^+$)	807
NH_2 (**2b**$^+$)	864		
	4-Pyrimidinamine		
N-1 (**3a**$^+$)	943	NH_2 (**3c**$^+$)	835
N-3 (**3b**$^+$)	905	C-5 (**3d**$^+$)	781

[a] In units of kJ mol^{-1}. Experimental value from ref 4.

Table 3. Dissociation Energies[a]

reaction	$\Delta H_{r,0}$ MP2[b]	$\Delta H_{r,0}$ B3LYP	$\Delta H_{r,298}$ MP2[b]	$\Delta H_{r,298}$ B3LYP
1 → **1d**$^\bullet$ + H$^\bullet$	448	435	454	441
1a$^\bullet$ → **1** + H$^\bullet$	74	117	77	120
1a$^\bullet$ (VN)[c] → **1** + H$^\bullet$	51	95		
1b$^\bullet$ (VN)[c] → **1** + H$^\bullet$	36	80		
2a$^\bullet$ → **2** + H$^\bullet$	79	112	84	116
2a$^\bullet$ (VN)[c] → **2** + H$^\bullet$	17	55		
2b$^\bullet$ (VN)[c] → **2** + H$^\bullet$	−106	−86		
2b$^\bullet$ (VN)[c] → **1d**$^\bullet$ + NH_3	−51	−81		
3a$^\bullet$ (VN)[c] → **3** + H$^\bullet$	−10	31		
3b$^\bullet$ (VN)[c] → **3** + H$^\bullet$	−12	33		

[a] In units of kJ mol^{-1}. [b] From spin projected MP2/6-311G(2d,p) energies and HF/6-31G(d,p) zero-point and thermal corrections. [c] From vertical neutralization of the cation.

cm^{-1}), and C−N stretching modes ($\nu_{N-1-C-2}$ = 1539 cm^{-1}). The Franck−Condon effects in neutralization of **1a**$^+$ were comparable to those in N-protonated pyridine (20 kJ mol^{-1}),[19] but much smaller than in N-protonated imidazole (185 kJ mol^{-1}).[16] The total spin densities in **1a**$^\bullet$, calculated by B3LYP/6-311G(2d,p), suggested that the radical can be represented by two dominant valence-bond canonical structures (Scheme 2).

Both MP2 and B3LYP gave positive, albeit different, dissociation thresholds for the loss of H-1 from **1a**$^\bullet$ (Table 3). The data in Table 3 and our previous calculations for the pyridine system[19] indicated that MP2 systematically underestimated the total energies of heterocyclic radicals by 30−40 kJ mol^{-1}, which resulted in dissociation energies which were too low by the same amount. This was probably due to spin contamination, which was substantial in the MP2 calculations and which was not completely eliminated by the spin projection method used.

While **1a**$^\bullet$ was found as a stable structure corresponding to a local potential energy minimum, its kinetic stability at energies above the dissociation threshold was also of interest. In addition to the Franck−Condon energy acquired upon vertical neutralization, **1a**$^\bullet$ must also contain a part of the vibrational energy introduced by the precursor cation. H_3O^+-protonated **1a**$^+$ can contain an average maximum of 207 kJ mol^{-1} vibrational energy from the protonation exothermicity (192 kJ mol^{-1}, eq 2) and the vibrational enthalpy of **1**, which was 14.7 kJ mol^{-1} at 475 K. This internal energy, if deposited in **1a**$^\bullet$, would exceed the calculated N-1−H-1 bond dissociation energy and should result in fast dissociation. The fact that a substantial fraction of **1a**$^\bullet$ survived even under conditions of highly exothermic protonation (Figure 1) pointed to the formation of vibrationally cooler **1a**$^\bullet$,

Scheme 2

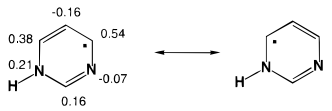

the presence of an activation barrier for the N-1−H-1 bond cleavage, or a combination of both. Collisional deexcitation undoubtedly occurred in a fraction of $\mathbf{1a}^+$ ions which were estimated to undergo 40−50 collisions with water molecules during the ion residence time in the ionization chamber. Conversely, excitation of the ring-breathing and C−N stretching vibrational modes in hot $\mathbf{1a}^+$ could result in a better geometry match between the precursor ion and relaxed $\mathbf{1a}^\bullet$, thus diminishing the Franck−Condon effects in a fraction of the radicals formed.[46] Regarding an activation barrier in the N−H bond cleavage, activation energies in radical additions and dissociations have been inferred previously for several systems. Shaik and Pross[47] employed their curve-crossing model to predict activation barriers on the order of 20−35 kJ mol^{-1} for radical additions to π-electronic systems in olefins.[48] Those barriers were due to interactions of the unpaired electron in the radical with the electron pair in the occupied π-orbital of the olefin.[48] For the present dissociation reaction, an activation barrier can be inferred from the correlation diagram shown in Figure 3. The odd electron in $\mathbf{1a}^\bullet$ occupies a SOMO π-orbital, which interacts only weakly with the doubly occupied σ-orbital of the N-1−H-1 bond. Homolytic cleavage of the σ-bond must therefore involve orbital mixing through $\pi \rightarrow \sigma^*$ or $\sigma \rightarrow \sigma^*$ excitation to allow electron reorganization and pairing in forming ground state **1**. Such excitations typically result in substantial activation barriers, as found, for example, for an analogous N−H bond cleavage in (3*H*)-imidazolinium radical.[16] Competing isomerizations, e.g., $\mathbf{1a}^\bullet \rightarrow \mathbf{1b}^\bullet$, were negligible in dissociating $\mathbf{1a}^\bullet$. The absence of competing isomerizations was very likely due to kinetic factors. Vertically neutralized $\mathbf{1b}^\bullet$ was calculated to be only 15 kJ mol^{-1} less stable than $\mathbf{1a}^\bullet$ toward loss of H, which should make $\mathbf{1b}^\bullet$ energetically accessible from dissociating $\mathbf{1a}^\bullet$. Therefore, the absence of $\mathbf{1a}^\bullet \rightarrow \mathbf{1b}^\bullet$ isomerization must be due to an activation barrier separating the isomers.

Protonation of 2-Pyrimidinamine. Protonation of **2**, followed by neutralization−reionization of stable $(\mathbf{2} + \mathrm{H})^+$ ions, produced fractions of survivor ions that depended on the protonation exothermicity. Figure 4 shows that the relative abundance of survivor $(\mathbf{2} + \mathrm{H})^+$ was lowest for the most exothermic protonation with CH_5^+ and increased for the less exothermic protonations with $C_4H_9^+$ and NH_4^+. Interestingly, the propensity for elimination of NH_3, relative to the loss of $\mathrm{H}^\bullet$, increased in the same series, as evidenced by the ion at *m/z* 79 (Figure 4). The question of protonation sites in **2** was addressed in three series of experiments. First, the active protons of the NH_2 group were exchanged for deuterium in solution, and the ND_2 derivative (**2**-d_2) was deuteronated in the gas phase with ND_4^+ and *t*-$C_4D_9^+$. Neutralization−reionization of the $(\mathbf{2}\text{-}d_2 + \mathrm{D})^+$ ions resulted in a clean loss of $\mathrm{D}^\bullet$ in both cases, as documented for the ND_4^+-deuteronated ions (Figure 5a). Hence, the C-4 through C-6 methines in **2** were not attacked by the gas-phase acids used. We also checked the neutralization−reionization spectrum of cation radical $\mathbf{2}\text{-}d_2^{\bullet+}$, which showed no detectable loss of H (<0.1%, Figure 5d). Loss of D from neutralized $(\mathbf{2}\text{-}d_2 + \mathrm{D})^+$ thus could not be simulated by consecutive losses of two light hydrogen atoms. Protonation of **2**-d_2 with *t*-$C_4H_9^+$, followed by neutralization−reionization, resulted in a dominant, but not exclusive, loss of $\mathrm{H}^\bullet$ (Figure 5c). In a complementary experiment, **2** was deuteronated with *t*-$C_4D_9^+$ to give $(\mathbf{2} + \mathrm{D})^+$, which was subjected to neutralization−reionization. The spectrum (Figure 5b) showed losses of $\mathrm{D}^\bullet$ and $\mathrm{H}^\bullet$ in a 2:1 ratio.

Product analysis based on radical dissociations allows one to determine the composition of a mixture of isomeric radicals and hence to assess the population of their precursor cations

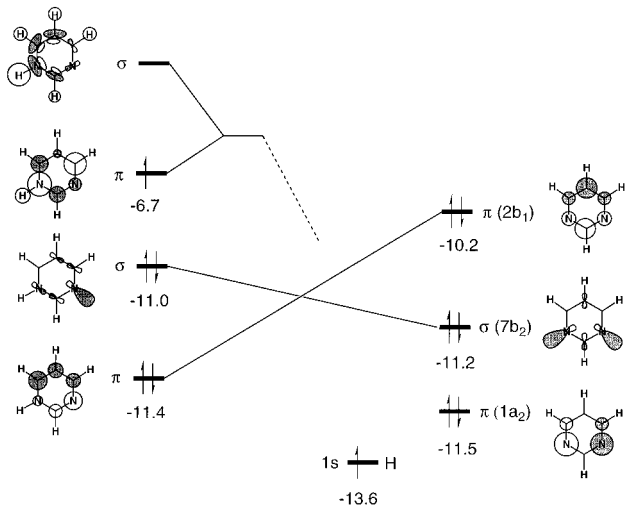

Figure 3. Orbital correlation diagram for the loss of hydrogen from $\mathbf{1a}^\bullet$. The orbital energies are in electronvolts.

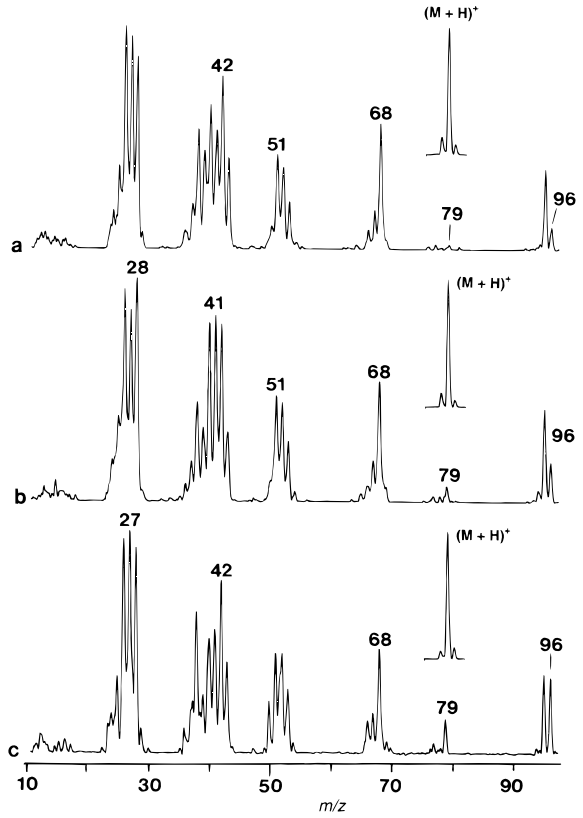

Figure 4. Neutralization (CH_3SSCH_3, 70% transmittance)−reionization (O_2, 70% transmittance) mass spectra of protonated 2-pyrimidinamine from protonations with (a) CH_5^+, (b) *t*-$C_4H_9^+$, and (c) NH_4^+. Insets show the $(\mathbf{2} + \mathrm{H})^+$ precursor ion relative intensities.

(46) (a) Nguyen, V. Q.; Shaffer, S. A.; Turecek, F.; Hop, C. E. C. A. *J. Phys. Chem.* **1995**, *99*, 15454. (b) Nguyen, V. Q.; Turecek, F. *J. Mass Spectrom.* **1996**, *31*, 843.

(47) (a) Pross, A.; Shaik, S. S. *Acc. Chem. Res.* **1983**, *16*, 363. (b) Shaik, S. S. *J. Mol. Liq.* **1994**, *61*, 49.

(48) Wong, M. W.; Pross, A.; Radom, L. *J. Am. Chem. Soc.* **1993**, *115*, 11050.

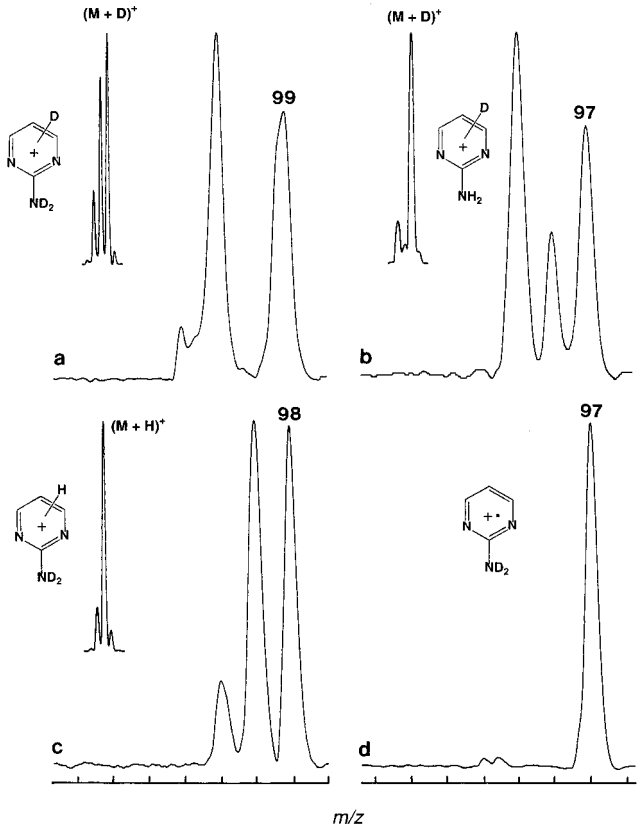

Figure 5. Partial NR mass spectra of 2-pyrimidinamine ions: (a) (**2**-d_2 + D) from deuteronation with ND_4^+; (b) (**2** + D)$^+$ from deuteronation with *t*-$C_4D_9^+$; (c) (**2**-d_2 + H)$^+$ from protonation with *t*-$C_4H_9^+$; (d) **2**-$d_2^{\bullet+}$. The collision conditions were as in Figure 1. Insets show the precursor ion relative intensities.

formed by protonation at different sites. Quantitative treatment of the relative abundances of the reionized products rests on several assumptions. First, it is assumed that the stable precursor cations have not isomerized by unimolecular hydrogen rearrangements. This is likely to be fulfilled for ion internal energies up to ca. 250 kJ mol^{-1}, which is the estimated energy barrier for proton migration in protonated aromates.[44] Second, the neutralization cross-sections are assumed to be similar for the isomeric cations and isotopomers. This is difficult to verify by experiment directly; however, the total neutralization−reionization yields for protonated and deuteronated **2** and **2**-d_2 were measured and found to be within ±30%, which is comparable to the reproducibility limits in NR cross-section measurements.[49] Third, the internal energy distributions in the isotopomers are presumed to be similar, such that the rates of competitive H/D losses are affected mostly by isotope effects.[50] Finally, the reionization cross-sections for the neutral products are presumed to be identical. This stems from the relative insensitivity of ionization cross-sections to the isomer structures in general,[51] and from the fact that the neutral products are isotopomers of **2**. The last two assumptions, which are common for most isotope analyses by mass spectrometry, are satisfied except for small molecules (H_2, CH_4), which show substantial isotope effects upon ionization.[52]

Given the absence of participation by the C-4 through C-6 methines, the relative intensities of the isotopomeric products could be fitted into mass-balance equations (eq 4−7)[16] to yield

$$0.833 = 2k_R \tag{4}$$

$$0.167 = 0.33k_A + (0.67/\alpha_{A1})k_A \tag{5}$$

$$0.667 = 2k_R/\alpha_R \tag{6}$$

$$0.333 = 0.67k_A/\alpha_{A2} + (0.33/\alpha_{A1})k_A \tag{7}$$

the relative rates for H$^\bullet$ loss from the ring N-1 or N-3 positions (k_R) and the NH_2 group (k_A), as well as the primary (α_R, α_{A1}) and secondary (α_{A2}) isotope effects on the H/D loss. A least-squares fit gave $k_R = 0.41$, $k_A = 0.38$, $\alpha_R = 1.23$, $\alpha_{A1} = 2.11$, and $\alpha_{A2} = 2.22$ with a root-mean-square deviation (rmsd) of 3% for the ion relative intensities. These data clearly showed that both the ring nitrogen atoms and the amino group were protonated with gaseous *t*-$C_4H_9^+$. Presuming that the relative rates for H$^\bullet$ loss represented the tautomer populations in (**2** + H)$^+$, one obtained 68% protonation at N-1 and N-3 and 32% protonation in the amino group.

The relative stabilities of protonated 2-pyrimidinamine tautomers were assessed by MP2/6-311G(2d,p) calculations, as summarized in Table 2. The calculations identified the N-1-protonated isomer **2a**$^+$ as the most stable isomer. The overall (thermodynamic) proton affinity of **2** was calculated at 909 kJ mol^{-1}. Compared with N-protonation in **1**, the substituent effect of the 2-amino group in **2** resulted in a proton affinity increase of 30 kJ mol^{-1}. This effect was greater than in the pyridine−2-aminopyridine system, where the 2-amino group caused a proton affinity increase of 12 kJ mol^{-1}.[4] Protonation at the amino group would create isomer **2b**$^+$, which was found to be 45 kJ mol^{-1} less stable than **1a**$^+$. The C-5 methine was even less basic, and its protonation would result in ion **2c**$^+$, which

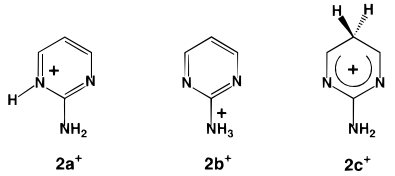

was 102 kJ mol^{-1} less stable than **2a**$^+$. In spite of its low absolute value, the proton affinity of the C-5 methine in **2** showed a large increase due to the effect of the 2-amino group, $\Delta PA = 162$ kJ mol^{-1}, when compared with C-5 in the parent pyrimidine system. This effect was greater than for the analogous C-4-protonation in aniline ($PA_{C-4} = 848$ kJ mol^{-1})[45] and benzene (PA = 753−759 kJ mol^{-1})[53], giving $\Delta PA = 89$−95 kJ mol^{-1}. The electronic effects are further discussed below.

The calculated proton affinities were in reasonable agreement with the experimental results. Protonations with *t*-$C_4H_9^+$ (PA(isobutane) = 802 kJ mol^{-1}) were substantially exothermic for both N-1 and/or N-3 ($\Delta PA = 107$ kJ mol^{-1}) and NH_2 ($\Delta PA = 62$ kJ mol^{-1}) and could be expected to occur with rate constants at the collisional limit,[12] which is typically reached at protonation exothermicities ≥20 kJ mol^{-1}.[54] Consequently, **2a**$^+$ and **2b**$^+$ should be produced in a nearly statistical 2:1 ratio, which was very close to that from the neutralization−reioniza-

(49) (a) Danis, P. O.; McLafferty, F. W. *Anal. Chem.* **1986**, *58*, 355. (b) Wesdemiotis, C.; Feng, R. *Org. Mass Spectrom.* **1988**, *23*, 416.

(50) Derrick, P. J. *Mass Spectrom. Rev.* **1983**, *2*, 285.

(51) (a) Fitch, W. L.; Sauter, A. D. *Anal. Chem.* **1983**, *55*, 832. (b) Turecek, F.; Brabec, L.; Hanus, V.; Zima, V.; Pytela, O. *Int. J. Mass Spectrom. Ion Processes* **1990**, *97*, 117.

(52) (a) Biemann, K. *Mass Spectrometry*; McGraw-Hill: New York, 1962. (b) Turecek, F. In *Applications of Mass Spectrometry to Organic Stereochemistry*, Splitter, J. S., Turecek, F., Eds.; VCH Publishers: New York, 1994; pp 674−680.

(53) The proton affinity of benzene was reported as 753 kJ mol^{-1} from refs 41 and 45 and 759 kJ mol^{-1} in ref 4.

(54) Bouchoux, G.; Salpin, J. Y.; Leblanc, D. *Int. J. Mass Spectrom. Ion Processes* **1996**, *153*, 37.

Scheme 3

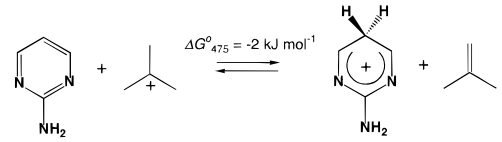

tion experiments (2.1:1).[55] Similar conclusions were reached previously for exothermic protonations of vicinal amino alcohols, in which the protonation sites were probed by stereospecific ion dissociations.[56] Protonation at C-5 was calculated to be only slightly exothermic at 298 K, and its thermodynamics was therefore investigated further at higher temperatures (Scheme 3). The calculated protonation exothermicity increased with temperature, e.g., from −5 to −9 kJ mol^{-1} at 298 and 600 K, respectively. However, the protonation entropy decreased in the same order from −9.7 to −14.6 J mol^{-1} K^{-1}. At the experimental temperature of 475 K, protonation at C-5 was only marginally exoergic (Scheme 3) and could not compete kinetically with protonations at N-1, N-3, or NH_2. Protonation with NH_4^+ was exothermic for N-1 and/or N-3 ($\Delta PA = 56$ kJ mol^{-1}) and the amino group ($\Delta PA = 11$ kJ mol^{-1}), so that all three nitrogen atoms could, in principle, be protonated. It is pertinent to note that in protonations with NH_4^+ the N-1, N-3, and NH_2 positions could not be distinguished by labeling because of an exchange of the amine protons with gas-phase ND_3. However, NR of ND_4^+-deuteronated **2** showed a clean loss of ND_3. This suggested the presence of a fraction of an ND_3 isomer (**2b**-d_3)$^+$, and/or a specific D transfer in the loss of ND_3 from **2a**-d_3^+.

2-Pyrimidinylammonium Radicals. Neutralization of ions **2a**$^+$ and **2b**$^+$ gave rise to isomeric radicals **2a**$^\bullet$ and **2b**$^\bullet$,

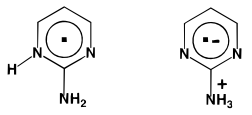

respectively, whose stabilities and dissociations were of interest. Computationally, **2a**$^\bullet$ was found to be a thermodynamically stable species both in its equilibrium geometry and following vertical reduction of **2a**$^+$. The dissociation by cleavage of the N-1−H bond was calculated to require 79−112 kJ mol^{-1} at 0 K according to MP2 and B3LYP, respectively. The corresponding Franck−Condon energies in vertically neutralized **2a**$^\bullet$ were estimated at 57−62 kJ mol^{-1} (Table 3). The optimized structures of **2a**$^+$ and **2a**$^\bullet$ gave a clue to the Franck−Condon effects; compared with **2a**$^+$, radical **2a**$^\bullet$ showed substantially elongated N-3−C-4, C-4−C-5, N-1−C-2, and N-1−C-6 bonds, whereas the C-2−N-3 bond was shortened. The other significant geometry features of neutral **2a**$^\bullet$ were the pyramidalizations at N-1 and the amine nitrogen (N-7), and, to a smaller extent, at C-2 as well. The bond lengths and the calculated total spin densities can be qualitatively depicted by canonical valence-

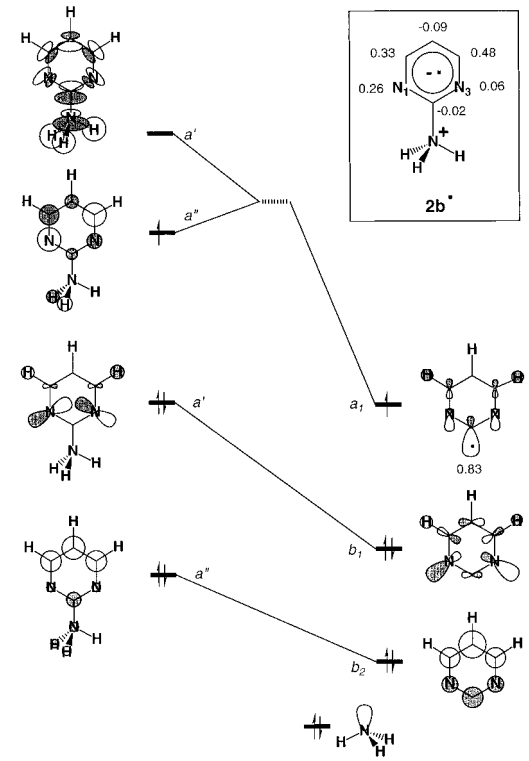

Figure 6. Orbital correlation diagram for the loss of ammonia from vertically reduced **2b**$^\bullet$. The inset shows the SCF total spin densities from a B3LYP/6-311G(2d,p) calculation.

Scheme 4

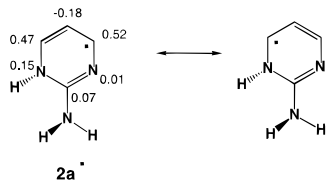

bond structures showing an interaction between the allylic radical π-system at C-4 through C-6 and the guanidine system of N-1, C-2, N-3, and N-7 (Scheme 4).

The ammonium radical **2b**$^\bullet$ was calculated to be thermodynamically unstable toward losses of the ammonium hydrogen atoms (H-7) and ammonia when formed by vertical neutralization of **2b**$^+$. These dissociations showed different relative exothermicities from MP2 and B3LYP calculations (Table 3), so that the exact energetics remained inconclusive. However, qualitative insight into the preferred dissociation of **2b**$^\bullet$ could be inferred from the total charge and spin densities and molecular-orbital analysis of the UHF and B3LYP/6-311G(2d,p) wave functions (Figure 6). The analysis revealed that the odd electron entered a π-type SOMO that was mostly localized in the pyrimidine ring (Figure 6). The electron populations pointed to **2b**$^\bullet$ being a highly polarized species in which the NH_3 group carried a partial positive charge (+0.46 by UHF, +0.45 by B3LYP) and the pyrimidine ring and hydrogen atoms a partial negative charge (−0.54 to −0.55). The total spin density was completely localized within the ring with major positive contributions from C-4 (0.48), C-6 (0.33), and N-1 (0.26) (Figure 6). Hence, the nascent **2b**$^\bullet$ can be depicted as a zwitterionic species consisting of the positively charged ammonium group and a negatively charged pyrimidine anion radical. This was very different from the electron distributions calculated previously for aliphatic ammonium radicals, which invariantly showed the odd electron to be located in a diffuse orbital of a

(55) A reviewer raised the question of local bond dipoles and their effect on the protonation topicity.[17] We note that the local dipoles for the N-1,3−C-2 and C-2−NH_2 bonds are similar due to the similar total atomic charges on N-1,3 (−0.393) and the amine N (−0.391), and the similar bond lengths for N-1,3−C-2 (1.329 Å) and C-2−NH_2 (1.316 Å). **2** has a small overall dipole moment, calculated as 0.44 D.

(56) (a) Longevialle, P.; Milne, G. W. A.; Fales, H. M. *J. Am. Chem. Soc.* **1973**, *95*, 6666. (b) Longevialle, P.; Girard, J. P.; Rossi, J. C.; Tichy, M. *Org. Mass Spectrom.* **1979**, *14*, 414. (c) Houriet, R.; Rufenacht, H.; Carrupt, P. A.; Vogel, P.; Tichy, M. *J. Am. Chem. Soc.* **1983**, *105*, 3417. (d) Houriet, R.; Rufenacht, H.; Stahl, D.; Tichy, M.; Longevialle, P. *Org. Mass Spectrom.* **1985**, *20*, 300.

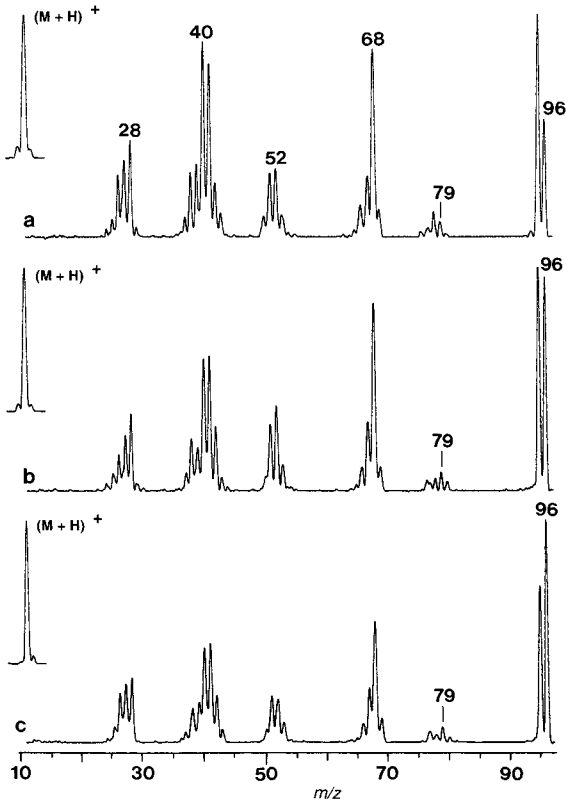

Figure 7. Neutralization (CH_3SSCH_3, 70% transmittance)−reionization (O_2, 70% transmittance) mass spectra of protonated 4-pyrimidinamine from protonations with (a) CH_5^+, (b) *t*-$C_4H_9^+$, and (c) NH_4^+. Insets show the $(\mathbf{3} + H)^+$ precursor ion relative intensities.

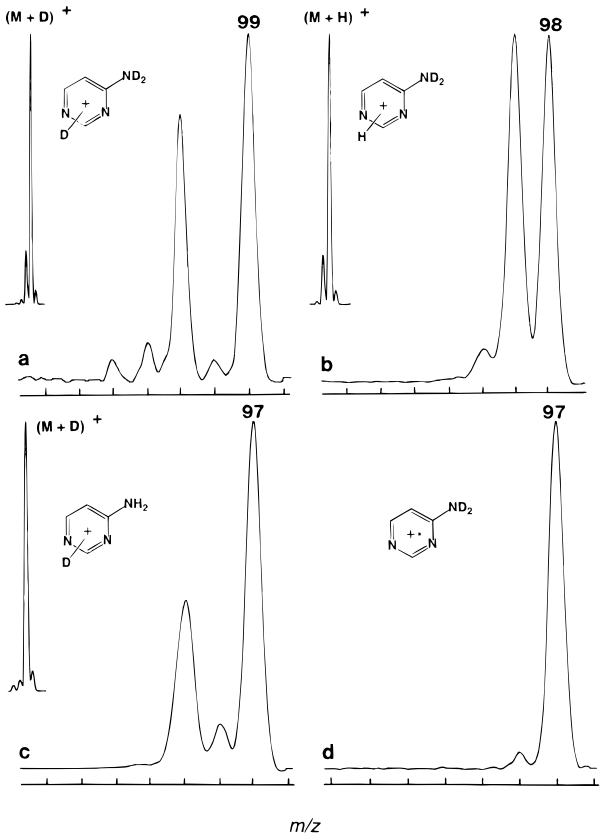

Figure 8. Partial NR mass spectra of 4-pyrimidinamine ions: (a) (**3**-d_2 + D)$^+$ from deuteronation with ND_4^+; (b) (**3**-d_2 + H)$^+$ from protonation with *t*-$C_4H_9^+$. (c) $(\mathbf{3} + D)^+$ from deuteronation with *t*-$C_4D_9^+$; (d) **3**-$d_2^{\bullet+}$. The collision conditions were as in Figure 1. Insets show the (M + H, D)$^+$ precursor ion relative intensities.

Rydberg or Rydberg-valence type and the N and H atoms to have substantial negative charge populations.[57]

Considering the elimination of ammonia from **2b**• by cleavage of the C-2−NH_3 bond, the orbital analysis showed that the SOMO π-orbital in **2b**• (a″) did not correlate by symmetry with the σ-type a_1 SOMO in the 2-pyrimidyl radical product **1d**• (Figure 6). A $\pi \rightarrow \sigma^*$ orbital mixing was necessary to achieve the correct frontier-orbital symmetry in the transition state. This may imply a potential energy barrier for the exothermic loss of NH_3, similar to the barriers predicted for N−C bond cleavages in aliphatic ammonium radicals.[57] By contrast, no involvement of excited states in **2b**• was necessary in the loss of one of the out-of-plane hydrogen atoms from the ammonium group to form **2**, because the HOMO in **2** was a π-type orbital which correlated with the a″ orbital in **2b**•. The presumed presence of an activation barrier for the N−C bond cleavage in **2b**• allowed us to interpret the observed loss of ammonia from $(\mathbf{2} + H)^+$ upon neutralization−reionization as being due to ion dissociations after reionization. Note that the loss of ammonia increased with decreasing precursor ion internal energy and with the increasing fraction of survivor $(\mathbf{2} + H)^+$. Interestingly, the behavior of **2b**• differed from that reported for protonated aniline, which instead showed an increased loss of ammonia upon neutralization−reionization of energetic ions.[58] The reason for this difference is not clear, because the electronic structure of the anilinium radical has not been studied. It is possible, however, that anilinium behaves like aliphatic hypervalent ammonium radicals in which the odd electron weakens both the N−H and N−C bonds.[57]

(57) (a) Shaffer, S. A.; Turecek, F. *J. Am. Chem. Soc.* **1994**, *116*, 8647. (b) Sadilek, M.; Turecek, F. *Chem. Phys. Lett.* **1996**, *263*, 203. (c) Nguyen, V. Q.; Sadilek, M.; Frank, A. J.; Ferrier, J. G.; Turecek, F. *J. Phys. Chem.*, submitted for publication.

(58) Nold, M. J.; Wesdemiotis, C. *J. Mass Spectrom.* **1996**, *31*, 1169.

Protonation of 4-Pyrimidinamine. The protonation sites in **3** were investigated using the same methodology as applied to **2**. Neutralization−reionization of $(\mathbf{3} + H)^+$ yielded remarkably abundant survivor ions that attested to an extraordinary stability of the intermediate $(\mathbf{3} + H)^\bullet$ radicals. For neutralization−reionization of NH_4^+-protonated **3**, the relative abundance of survivor $(\mathbf{3} + H)^+$ was greater than that for survivor $\mathbf{3}^{\bullet+}$ from NR of the 4-pyrimidinamine cation radical! Substantial survivor ions were recovered even for $(\mathbf{3} + H)^+$ prepared by the highly exothermic protonation with CH_5^+ (Figure 7). Loss of H• (*m/z* 95) and ring cleavages were the main dissociation pathways of $(\mathbf{3} + H)^+$ upon neutralization−reionization (Figure 7).

Neutralization−reionization of (**3**-d_2 + D)$^+$ resulted in a dominant loss of deuterium (Figure 8a). This distinguished the N-1, N-3 and NH_2 positions from the C-2, C-5, and C-6 methines and showed that the latter were not deuteronated efficiently by gas-phase ND_4^+. NR of $(\mathbf{3} + D)^+$ from deuteronation with *t*-$C_4D_9^+$ resulted in a predominant loss of D• (Figure 8c), which distinguished N-1 and N-3 from the NH_2 group. Likewise, protonation with *t*-$C_4H_9^+$ of the ND_2 derivative **3**-d_2, followed by NR of the (**3**-d_2 + H)$^+$ ion, resulted in a major loss of light hydrogen (95%, Figure 8b). The relative intensity of the (**3**-d_2 + H − D)$^+$ in the spectrum of (**3**-d_2 + H)$^+$ was corrected for the small contribution (<3%) from the peak due to H loss from **3**-d_2, which overlapped at *m/z* 96 (Figure 8b,d). Dominant protonation of the ring nitrogens was thus indicated by labeling.

To quantify the NR data, the fractions for loss of H• and D• from the isotopomers were fitted to mass-balance equations (eqs 8−13), where k_N, k_A, and k_C were the relative rates for H• loss

$$0.927 = k_N/\alpha_N + 3k_A/\alpha_A + k_C/2\alpha_C \quad (8)$$

$$0.073 = k_C/2 \quad (9)$$

$$0.948 = k_N + k_C + k_A/3\alpha_A \quad (10)$$

$$0.052 = 2k_A/3 \quad (11)$$

$$0.787 = k_C/2\alpha_C + k_N/\alpha_N + k_A/3\alpha_A \quad (12)$$

$$0.213 = k_C/2 + 2k_A/3 \quad (13)$$

from the ring nitrogens (N-1 and N-3), amino group, and ring carbon positions (C-2, C-5, and C-6), respectively, and α_N, α_A, and α_C are the respective primary isotope effects. Because the individual ring positions were not resolved by specific labeling in this case, only total fractions for the ring nitrogens and methines and average primary isotope effects could be obtained, whereas secondary isotope effects were neglected. The least-squares fit gave $k_N = 0.82$, $k_A = 0.12$, $k_C = 0.13$, $\alpha_N = 1.2$, $\alpha_A = 1.65$, and $\alpha_C = 1.0$ with a 3.6% rmsd. This showed a major, but not exclusive, loss from the ring nitrogen positions of protons or deuterons introduced by the gas-phase acid. Hence, predominant protonation at N-1 and/or N-3 was strongly indicated.

The protonation energetics and stabilities of $(\mathbf{3} + H)^\bullet$ radicals were further addressed by ab initio calculations (Table 3). **3** was found to be 7 and 9 kJ mol^{-1} less stable than **2** at 298 K by MP2 and B3LYP, respectively. However, **3** was found to be substantially more basic than **2**. N-1 was calculated to be the most basic site in **3**, which showed a thermodynamic proton affinity of 943 kJ mol^{-1}. The proton affinity of N-3 (905 kJ mol^{-1}) was similar to that of N-1 and/or N-3 in **2** (Table 2). By contrast, the amino group and the C-5 methine in **3** were less basic than the equivalent positions in **2** (Table 2). The proton affinities further showed that the ring nitrogen atoms and the amino group should be attacked exothermically by *t*-$C_4H_9^+$, whereas C-5 should not. Protonation with NH_4^+ was exothermic for the ring nitrogens only. The thermodynamics for protonation at C-5 with *t*-$C_4H_9^+$ (Scheme 5) was further checked by calculating the reaction free energies ($\Delta G°_T$) in the 298−600 K range, which included the experimental protonation temperatures of 450−495 K. The calculated $\Delta H°_T$ showed a decrease from 21 to 18 kJ mol^{-1} at 298 and 600 K, respectively. However, this was compensated by a reaction entropy decrease from −4.3 to −8.4 kJ mol^{-1} K^{-1} at 298 and 600 K, respectively, resulting in a positive $\Delta G°_{475}$ for the reaction (Scheme 5). Hence, protonation by *t*-$C_4H_9^+$ at C-5 in **3** was thermodynamically disfavored at any relevant experimental temperature.

Comparison of the calculated proton affinities with the experimental data for **3** showed an overall agreement but also pointed out some apparent discrepancies. The experiment and theory agreed on the preferential protonation of N-1 and N-3 in **3**. The small fraction of the NH_2-protonated isomer ($\mathbf{3c}^+$)

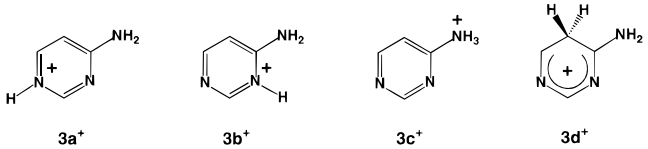

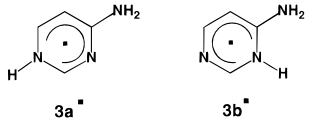

Scheme 5

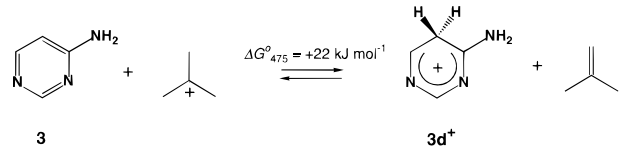

was also consistent with the low exothermicity calculated for protonation with *t*-$C_4H_9^+$. However, protonation at C-5 should not be energetically feasible, and yet the experiment indicated that the carbon positions were involved in the radical and/or ion dissociations. Could the other carbon positions in **3** be protonated with *t*-$C_4H_9^+$? The basicities of C-2 and C-6 are affected by the σ-acceptor effects of the ring nitrogen atoms and the π-donor effect of the amino group.[1] The former effect decreases the electron density in the ortho and para positions (C-2 and C-6) more efficiently than in the meta position C-5.[1] Accordingly, C-2 is 72 kJ mol^{-1} less basic than C-5 in **1**. The effect of the amino group in **2** and **3** is quite analogous to the directional effects in electrophilic substitution[1,59] in that it enhances the basicity of the ortho and para positions, e.g., C-5 in **2**. A combination of these two effects in **3** is positively cumulative for protonation at C-5 and negatively cumulative for positions C-2 and C-6. Hence, C-5 should be the most basic carbon atom in **3**.

It follows that the minor loss of H$^\bullet$ from C-2 through C-6 upon NR did not originate from isomers formed by specific protonation of the ring carbons. As discussed previously for other nitrogen heterocycles,[16,19] hydrogen migrations in survivor ions can obscure the protonation sites and result in losses of hydrogen atoms from positions that were not protonated in the precursor ion. Alternatively, C−H bond cleavage can occur in energetic radicals or ions to yield less stable ylide or ylidion isomers.[44b] For **3**, it appears probable that the loss of the ring hydrogens occurred in a fraction of reionized $(\mathbf{3} + H)^+$ ions, which were abundant in the spectra and which received additional energy upon collisional reionization.[46b,60] It is pertinent to note in this context that collision-induced dissociation of $(\mathbf{3} + H)^+$ did result in loss of H$^\bullet$. Hydrogen migrations in aromatic and heterocyclic cations have been estimated to have activation barriers of 240−260 kJ mol^{-1},[44] which were substantially less than the N−H bond dissociation energies, e.g., 505 kJ mol^{-1} in N-protonated pyridine.[19] High-energy, dissociating ions therefore could undergo hydrogen scrambling that preceded the hydrogen loss.[17,18]

Vertical neutralization of $\mathbf{3a}^+$ and $\mathbf{3b}^+$ formed the corresponding radicals, which were found to be thermodynamically stable by B3LYP, whereas the MP2 energies predicted exothermic dissociation for $\mathbf{3a}^\bullet$ and $\mathbf{3b}^\bullet$ (Table 3). Unfortunately, $(\mathbf{3} + H)^\bullet$ isomers lack molecular symmetry which made the calculations with the 6-311G(2d,p) basis set time consuming beyond our computational capabilities. Therefore, optimized structures and total energies could not be obtained at an appropriate level of theory. Judged from the spectrometric data (Figure 7), $\mathbf{3a}^\bullet$ and $\mathbf{3b}^\bullet$ must be kinetically stable to give rise to the very large fractions of the survivor ions observed. It is noteworthy that kinetically stable radicals were obtained even from vibrationally excited precursor cations that were prepared by the highly exothermic protonation with CH_5^+ (Figure 7a) which can deposit up to ∼400 kJ mol^{-1} in $\mathbf{3a}^+$, as estimated from the difference in the corresponding proton affinities. This

(59) March J. *Advanced Organic Chemistry*, 3rd ed.; Wiley-Interscience: New York, 1985; pp 447−463.
(60) Beranova, S.; Wesdemiotis, C. *J. Am. Soc. Mass Spectrom.* **1994**, *5*, 1093.

implies that, in addition to their thermodynamic stabilities, **3a**• and/or **3b**• must also be stabilized kinetically by substantial activation barriers to N−H bond dissociations.

Conclusions

Neutralization−reionization experiments and ab initio theory agreed on the ring nitrogen atoms being the most basic sites in gaseous pyrimidine and pyrimidinamines. The amino group in pyrimidinamines increased the basicity of the ring nitrogen atoms by π-donation. This effect was notably greater for the para nitrogen atom in **3** than for the ortho nitrogen atoms in **2** and **3**. The pyrimidine ring exerted an electron-withdrawing effect on the amino groups in **2** and **3**, which showed lower topical proton affinities than the amino group in aniline.

Vertical neutralization of protonated **1**, **2**, and **3** yielded radicals which were both thermodynamically and kinetically stable. The ring-protonated isomer **2a**• was found to be stable when formed by vertical neutralization. Vertical neutralization of protonated **3** formed pyrimidinium radicals which showed unusual kinetic stability toward loss of hydrogen atom.

Acknowledgment. Support by the National Science Foundation (Grant CHE-9412774) and the ACS Petroleum Research Fund is gratefully acknowledged. The ab initio calculations were conducted by using the resources of the Cornell Theory Center, which receives major funding from the National Science Foundation and New York State, with additional support from the Advanced Research Projects Agency, the National Center for Research Resources at the National Institutes of Health, IBM Corp., and members of the Corporate Research Institute. We also thank Dr. Jan E. Szulejko for providing us with a critically evaluated list of proton affinities and Dr. Graham McGibbon for communicating his results on pyridine ylides prior to publication.

Supporting Information Available: Tables of optimized geometries as Cartesian coordinates and uncorrected harmonic frequencies (8 pages). See any current masthead page for ordering and Internet access instructions.

JA9634785